

HIGHER ORDER TRACE FINITE ELEMENT METHODS FOR THE SURFACE STOKES EQUATION

THOMAS JANKUHN* AND ARNOLD REUSKEN†

Abstract. In this paper a class of higher order finite element methods for the discretization of surface Stokes equations is studied. These methods are based on an unfitted finite element approach in which standard Taylor-Hood spaces on an underlying bulk mesh are used. For treating the constraint that the velocity must be tangential to the surface a penalty method is applied. Higher order geometry approximation is obtained by using a parametric trace finite element technique, known from the literature on trace finite element methods for scalar surface partial differential equations. Based on theoretical analyses for related problems, specific choices for the parameters in the method are proposed. Results of a systematic numerical study are included in which different variants are compared and convergence properties are illustrated.

Key words. surface Stokes equation, trace finite element method, Taylor-Hood finite elements

1. Introduction. In recent years there has been a strongly growing interest in the field of modeling and numerical simulation of surface fluids, cf. the papers [2, 14, 16, 22, 23, 31], in which Navier-Stokes type PDEs on (evolving) surfaces are treated. Navier-Stokes equations posed on manifolds is a classical topic in analysis, cf., e.g., [9, 21, 34, 35]. There are only very few papers that study numerical methods for surface (Navier-)Stokes equations [24, 31, 30, 32, 10, 25, 28, 3, 27, 17]. Most of these papers consider either a (Navier-)Stokes system in stream function formulation (which assumes that the surface is simply connected) or use low order \mathbf{P}_1 - P_1 finite elements, combined with stabilization techniques. As far as we know, [10, 27, 17] are the only papers in which higher order finite element methods for surface Navier-Stokes equations are studied. In [10] a surface finite element approach [8] is used and the condition that the velocity must be tangential to the surface is enforced weakly by a Lagrange multiplier approach. In [17] a surface finite element approach is combined with a Piola transformation for the construction of divergence-free tangential finite elements. In [27] stability of a variant of the \mathbf{P}_2 - P_1 Taylor-Hood pair for surface Stokes equations is analyzed and optimal discretization error bounds are derived. In this paper we consider a higher order finite element discretization that is based on a trace approach as in [27]. For treating the tangential condition we use a penalty approach instead of the Lagrange multiplier method that is used in [10]. Instead of the surface finite element method of [10] we use a so-called trace finite element method. For scalar elliptic surface partial differential equations the surface and trace approaches are explained and compared in [4]. The former technique essentially uses an explicit surface triangulation with surface finite element spaces defined on it, whereas the latter approach uses an implicit (e.g., level set) representation of the surface combined with finite element spaces that are defined on an underlying unfitted bulk mesh.

The trace finite element method is a geometrically *unfitted* discretization. In

*Institut für Geometrie und Praktische Mathematik, RWTH-Aachen University, D-52056 Aachen, Germany (jankuhn@igpm.rwth-aachen.de)

†Institut für Geometrie und Praktische Mathematik, RWTH-Aachen University, D-52056 Aachen, Germany (reusken@igpm.rwth-aachen.de).

particular in a setting with evolving surfaces $\Gamma(t)$ such unfitted finite element techniques, also called cut FEM, have certain attractive properties concerning flexibility (no remeshing) and robustness (w.r.t. handling of topological singularities); see [26, 5] for an overview of these techniques.

In this paper we study a trace variant of the Taylor-Hood pair \mathbf{P}_k-P_{k-1} , $k \geq 2$, for discretization of surface Stokes equations. The case $k = 2$ is treated in [27]. Compared to Stokes equations in Euclidean domains, the surface variant leads to several additional issues that have to be addressed. The two most important issues are the following:

1. *Tangential flow constraint.* In surface flow problems the flow has to be tangential to the surface. It is not obvious how this constraint (which is trivially satisfied in Euclidean domains) can be treated numerically. A technique used in several recent papers is as follows: the surface PDE for the tangential flow field is replaced by a PDE that allows fully three-dimensional velocities, defined on the surface, and a penalty approach is used to control the component of the velocity field that is normal to the surface.

2. *Sufficiently accurate geometry approximation.* This topic resembles the problem of a sufficiently accurate boundary approximation for (Navier-)Stokes equations in Euclidean domains. For the latter the isoparametric finite element technique is a standard approach. It is evident that for the case in which the domain is a curved surface the issue of geometry approximation becomes much more important. To state it differently, for problems in Euclidean domains with a polygonal boundary, standard higher order finite elements (e.g., Taylor-Hood pair) yield optimal higher order accuracy, whereas in a finite element method for surface PDEs one *always* needs a “sufficiently accurate” surface approximation for optimal higher order accuracy.

As mentioned above, we restrict to trace finite element techniques. Already for the case of scalar surface PDEs, in such trace methods one applies an appropriate stabilization to control instabilities caused by “small cuts”.

In this setting of trace finite element methods for surface Stokes equations several important questions arise that are non-existent in Stokes problems in Euclidean domains. For example, how does the error in the geometry approximation influence the discretization error, or, what is an appropriate scaling (in terms of the mesh size parameter h) of the penalty and stabilization parameters?

For the trace variant of the Taylor-Hood pair that we present in this paper for all parameters, such as the order of polynomial degree used in the geometry approximation, the penalty parameter and stability parameters, specific choices are proposed. These are based on analyses of related problems presented in [15, 27]. In [15] an error analysis of a class of higher order trace finite element methods for a surface vector-Laplace problem is given. In [27] the discrete inf-sup stability of a trace \mathbf{P}_2-P_1 Taylor-Hood pair is derived.

Key ingredients of the higher order trace finite element methods that we present in this paper are the following:

- We use a penalty formulation for treating the tangential constraint. Two different variants will be studied, namely a consistent and an inconsistent one. Precise explanations are given in Section 3.

- We use parametric trace finite element spaces, known from scalar surface PDEs [11] and higher order unfitted FEM for interface problems [20], to obtain a higher order geometry approximation. The basic idea of this technique is outlined in Section 4.
- The resulting trace finite element methods, including appropriate stabilization terms, are presented in Section 5. The stabilization that we use, is the so-called *volume normal derivative* stabilization, known from the literature.

To decide on appropriate parameter choices, we briefly recall recently obtained rigorous stability and discretization error results for \mathbf{P}_2 - P_1 surface Taylor-Hood elements [27] and error bounds for trace FEM applied to surface vector-Laplace equations [15]. These results are given in Section 6. The proposed methods are applied to a surface Stokes equation on a sphere and on a torus. Results of numerical experiments that illustrate the optimal order of accuracy in different norms are presented in Section 7.

The topic of this paper relates to the one in [27] as follows. In the latter paper the focus is on a theoretical analysis of discrete inf-sup stability of the trace \mathbf{P}_2 - P_1 Taylor-Hood pair. An optimal order discretization error bound for this pair is derived in which, however, geometry errors are not treated. In this paper we focus on a general methodology for higher order trace \mathbf{P}_k - P_{k-1} Taylor-Hood pairs, $k \geq 2$, in which the issue of geometry errors is also addressed. Furthermore, we compare two different penalty approaches, namely a consistent and an inconsistent one.

2. Continuous problem. We assume that $\Omega \subset \mathbb{R}^3$ is a polygonal domain which contains a connected compact smooth hypersurface Γ without boundary. For the higher order finite element method that we introduce below it is essential that the surface Γ is characterized as the zero level of a smooth level set function. For this we introduce some notation. A tubular neighborhood of Γ is denoted by $U_\delta := \{x \in \mathbb{R}^3 \mid |d(x)| < \delta\}$, with $\delta > 0$ and d the signed distance function to Γ , which we take negative in the interior of Γ . The surface Γ is (implicitly) represented as the zero level of a smooth level set function $\phi: U_\delta \rightarrow \mathbb{R}$, i.e.

$$\Gamma = \{x \in \Omega \mid \phi(x) = 0\}.$$

This level set function is not necessarily close to a distance function but has the usual properties of a level set function:

$$\|\nabla\phi(x)\| \sim 1, \quad \|\nabla^2\phi(x)\| \leq c \quad \text{for all } x \in U_\delta.$$

We assume that the level set function ϕ is sufficiently smooth. On U_δ we define $\mathbf{n}(x) = \nabla d(x)$, the outward pointing unit normal on Γ , $\mathbf{H}(x) = \nabla^2 d(x)$, the Weingarten map, $\mathbf{P} = \mathbf{P}(x) := \mathbf{I} - \mathbf{n}(x)\mathbf{n}(x)^T$, the orthogonal projection onto the tangential plane, $p(x) = x - d(x)\mathbf{n}(x)$, the closest point projection. We assume $\delta > 0$ to be sufficiently small such that the decomposition $x = p(x) + d(x)\mathbf{n}(x)$ is unique for all $x \in U_\delta$. The constant normal extension for vector functions $\mathbf{v}: \Gamma \rightarrow \mathbb{R}^3$ is defined as $\mathbf{v}^e(x) := \mathbf{v}(p(x))$, $x \in U_\delta$. The extension for scalar functions is defined similarly. Note that on Γ we have $\nabla \mathbf{v}^e = \nabla(\mathbf{v} \circ p) = \nabla \mathbf{v}^e \mathbf{P}$, with $\nabla \mathbf{w} := (\nabla w_1, \nabla w_2, \nabla w_3)^T \in \mathbb{R}^{3 \times 3}$ for smooth vector functions $\mathbf{w}: U_\delta \rightarrow \mathbb{R}^3$. For a scalar function $g: U_\delta \rightarrow \mathbb{R}$ and a vector

function $\mathbf{v}: U_\delta \rightarrow \mathbb{R}^3$ we define the surface (tangential and covariant) derivatives by

$$\begin{aligned}\nabla_\Gamma g(x) &= \mathbf{P}(x)\nabla g(x), \quad x \in \Gamma, \\ \nabla_\Gamma \mathbf{v}(x) &= \mathbf{P}(x)\nabla \mathbf{v}(x)\mathbf{P}(x), \quad x \in \Gamma.\end{aligned}$$

If g, \mathbf{v} are defined only on Γ , we use these definitions applied to the extension g^e, \mathbf{v}^e . On Γ we consider the surface stress tensor (see [12]) given by

$$E_s(\mathbf{u}) := \frac{1}{2} (\nabla_\Gamma \mathbf{u} + \nabla_\Gamma^T \mathbf{u}),$$

with $\nabla_\Gamma^T \mathbf{u} := (\nabla_\Gamma \mathbf{u})^T$. To simplify the notation we write $E = E_s$. The surface divergence operator for vector-valued functions $\mathbf{u}: \Gamma \rightarrow \mathbb{R}^3$ and tensor-valued functions $\mathbf{A}: \Gamma \rightarrow \mathbb{R}^{3 \times 3}$ are defined as

$$\begin{aligned}\operatorname{div}_\Gamma \mathbf{u} &:= \operatorname{tr}(\nabla_\Gamma \mathbf{u}), \\ \operatorname{div}_\Gamma \mathbf{A} &:= (\operatorname{div}_\Gamma(\mathbf{e}_1^T \mathbf{A}), \operatorname{div}_\Gamma(\mathbf{e}_2^T \mathbf{A}), \operatorname{div}_\Gamma(\mathbf{e}_3^T \mathbf{A}))^T,\end{aligned}$$

with \mathbf{e}_i the i th basis vector in \mathbb{R}^3 . For a given force vector $\mathbf{f} \in L^2(\Gamma)^3$, with $\mathbf{f} \cdot \mathbf{n} = 0$, and a source term $g \in L^2(\Gamma)$, with $\int_\Gamma g \, ds = 0$, we consider the following *surface Stokes problem*: determine $\mathbf{u}: \Gamma \rightarrow \mathbb{R}^3$ with $\mathbf{u} \cdot \mathbf{n} = 0$ and $p: \Gamma \rightarrow \mathbb{R}$ with $\int_\Gamma p \, ds = 0$ such that

$$\begin{aligned}-\mathbf{P} \operatorname{div}_\Gamma(E(\mathbf{u})) + \mathbf{u} + \nabla_\Gamma p &= \mathbf{f} && \text{on } \Gamma, \\ \operatorname{div}_\Gamma \mathbf{u} &= g && \text{on } \Gamma.\end{aligned}\tag{2.1}$$

We added the zero order term on the left-hand side to avoid technical details related to the kernel of the strain tensor E (the so-called Killing vector fields). The surface Sobolev space of weakly differentiable vector valued functions is denoted by

$$\mathbf{V} := H^1(\Gamma)^3, \quad \text{with } \|\mathbf{u}\|_{H^1(\Gamma)}^2 := \int_\Gamma \|\mathbf{u}(s)\|_2^2 + \|\nabla \mathbf{u}^e(s)\|_2^2 \, ds.\tag{2.2}$$

The corresponding subspace of *tangential* vector field is denoted by

$$\mathbf{V}_T := \{\mathbf{u} \in \mathbf{V} \mid \mathbf{u} \cdot \mathbf{n} = 0\}.$$

A vector $\mathbf{u} \in \mathbf{V}$ can be orthogonally decomposed into a tangential and a normal part. We use the notation:

$$\mathbf{u} = \mathbf{P}\mathbf{u} + (\mathbf{u} \cdot \mathbf{n})\mathbf{n} = \mathbf{u}_T + u_N \mathbf{n}.$$

For $\mathbf{u}, \mathbf{v} \in \mathbf{V}$ and $p \in L^2(\Gamma)$ we introduce the bilinear forms

$$a(\mathbf{u}, \mathbf{v}) := \int_\Gamma E(\mathbf{u}) : E(\mathbf{v}) \, ds + \int_\Gamma \mathbf{u} \cdot \mathbf{v} \, ds,\tag{2.3}$$

$$b_T(\mathbf{u}, p) := - \int_\Gamma p \operatorname{div}_\Gamma \mathbf{u}_T \, ds.\tag{2.4}$$

Note that in the definition of $b_T(\mathbf{u}, p)$ only the *tangential* component of \mathbf{u} is used, i.e., $b_T(\mathbf{u}, p) = b_T(\mathbf{u}_T, p)$ for all $\mathbf{u} \in \mathbf{V}, p \in L^2(\Gamma)$. This property motivates the notation $b_T(\cdot, \cdot)$ instead of $b(\cdot, \cdot)$. If p is from $H^1(\Gamma)$, then integration by parts yields

$$b_T(\mathbf{u}, p) = \int_\Gamma \mathbf{u}_T \cdot \nabla_\Gamma p \, ds = \int_\Gamma \mathbf{u} \cdot \nabla_\Gamma p \, ds.\tag{2.5}$$

We introduce the following variational formulation of (2.1): determine $(\mathbf{u}_T, p) \in \mathbf{V}_T \times L_0^2(\Gamma)$ such that

$$\begin{aligned} a(\mathbf{u}_T, \mathbf{v}_T) + b_T(\mathbf{v}_T, p) &= (\mathbf{f}, \mathbf{v}_T)_{L^2(\Gamma)} \quad \text{for all } \mathbf{v}_T \in \mathbf{V}_T, \\ b_T(\mathbf{u}_T, q) &= (-g, q)_{L^2(\Gamma)} \quad \text{for all } q \in L^2(\Gamma). \end{aligned} \quad (2.6)$$

The bilinear form $a(\cdot, \cdot)$ is continuous on \mathbf{V} , hence on \mathbf{V}_T . The ellipticity of $a(\cdot, \cdot)$ on \mathbf{V}_T follows from the following surface Korn inequality, that holds if Γ is C^2 smooth ((4.8) in [14]): There exists a constant $c_K > 0$ such that

$$\|\mathbf{u}\|_{L^2(\Gamma)} + \|E(\mathbf{u})\|_{L^2(\Gamma)} \geq c_K \|\mathbf{u}\|_{H^1(\Gamma)} \quad \text{for all } \mathbf{u} \in \mathbf{V}_T. \quad (2.7)$$

The bilinear form $b_T(\cdot, \cdot)$ is continuous on $\mathbf{V}_T \times L_0^2(\Gamma)$ and satisfies the following inf-sup condition (Lemma 4.2 in [14]): There exists a constant $c > 0$ such that estimate

$$\inf_{p \in L_0^2(\Gamma)} \sup_{\mathbf{v}_T \in \mathbf{V}_T} \frac{b_T(\mathbf{v}_T, p)}{\|\mathbf{v}_T\|_{H^1(\Gamma)} \|p\|_{L^2(\Gamma)}} \geq c,$$

holds. Hence, the weak formulation (2.6) is a *well-posed problem*. The unique solution is denoted by (\mathbf{u}_T^*, p^*) . The main topic of this paper will be a class of higher order finite element methods for the discretization of this surface Stokes problem.

3. Treatment of tangential flow constraint. The weak formulation (2.6) is not very suitable for a Galerkin finite element discretization, because we would need finite element functions that are (approximately) tangential to Γ . Recently, very useful penalty approaches have been introduced [14, 13, 15]. These techniques allow a full three-dimensional velocity \mathbf{u} (not necessarily tangential to Γ) and penalize the normal component of \mathbf{u} . An alternative approach that avoids penalization has recently been introduced in [3].

In this section we recall two known penalty formulations: a consistent formulation and an inconsistent one. These are formulated as well-posed variational problems in a Hilbert space that contains \mathbf{V}_T . In section 5 we apply a Galerkin discretization (modulo geometric errors) to these variational formulations. Both resulting finite element methods have their own merits, cf. Section 8.

We define $\mathbf{V}_* \supset \mathbf{V} \supset \mathbf{V}_T$:

$$\mathbf{V}_* := \{\mathbf{u} \in L^2(\Gamma)^3 \mid \mathbf{u}_T \in \mathbf{V}_T, u_N \in L^2(\Gamma)\}, \quad \|\mathbf{u}\|_{\mathbf{V}_*}^2 := \|\mathbf{u}_T\|_{H^1(\Gamma)}^2 + \|u_N\|_{L^2(\Gamma)}^2.$$

Based on the identity

$$E(\mathbf{u}) = E(\mathbf{u}_T) + u_N \mathbf{H}, \quad \mathbf{u} \in \mathbf{V}, \quad (3.1)$$

we introduce an extension of the bilinear form $a(\cdot, \cdot)$ from \mathbf{V} to the larger space \mathbf{V}_* :

$$a(\mathbf{u}, \mathbf{v}) := \int_{\Gamma} (E(\mathbf{u}_T) + u_N \mathbf{H}) : (E(\mathbf{v}_T) + v_N \mathbf{H}) ds + \int_{\Gamma} \mathbf{u} \cdot \mathbf{v} ds, \quad \mathbf{u}, \mathbf{v} \in \mathbf{V}_*. \quad (3.2)$$

This bilinear form is well-defined and continuous on \mathbf{V}_* . We also define a penalty bilinear form

$$k(\mathbf{u}, \mathbf{v}) := \eta \int_{\Gamma} (\mathbf{u} \cdot \mathbf{n}) (\mathbf{v} \cdot \mathbf{n}) ds \quad \mathbf{u}, \mathbf{v} \in \mathbf{V}_*,$$

with $\eta > 0$ a penalty parameter, and

$$A(\mathbf{u}, \mathbf{v}) := a(\mathbf{u}, \mathbf{v}) + k(\mathbf{u}, \mathbf{v}) \quad \mathbf{u}, \mathbf{v} \in \mathbf{V}_*.$$

We further introduce the bilinear form $a_T(\cdot, \cdot)$ in which only the tangential components of the arguments play a role:

$$a_T(\mathbf{u}, \mathbf{v}) := a(\mathbf{P}\mathbf{u}, \mathbf{P}\mathbf{v}) = a(\mathbf{u}_T, \mathbf{v}_T), \quad (3.3)$$

and correspondingly,

$$A_T(\mathbf{u}, \mathbf{v}) := a_T(\mathbf{u}, \mathbf{v}) + k(\mathbf{u}, \mathbf{v}) \quad \mathbf{u}, \mathbf{v} \in \mathbf{V}_*.$$

(Note that $A(\cdot, \cdot)$ and $A_T(\cdot, \cdot)$ depend on the penalty parameter η). A *consistent* penalty surface Stokes formulation is: Determine $(\mathbf{u}, p) \in \mathbf{V}_* \times L_0^2(\Gamma)$ such that

$$\begin{aligned} A_T(\mathbf{u}, \mathbf{v}) + b_T(\mathbf{v}, p) &= (\mathbf{f}, \mathbf{v})_{L^2(\Gamma)} \quad \text{for all } \mathbf{v} \in \mathbf{V}_*, \\ b_T(\mathbf{u}, q) &= -(g, q)_{L^2(\Gamma)} \quad \text{for all } q \in L^2(\Gamma). \end{aligned} \quad (\text{P1})$$

Using the surface Korn inequality (2.7) one obtains ellipticity of the bilinear form $A_T(\cdot, \cdot)$, which is used to derive the following result (Theorem 6.1 in [14]):

LEMMA 3.1. *Problem (P1) is well-posed. For the unique solution $(\tilde{\mathbf{u}}, \tilde{p}) \in \mathbf{V}_* \times L_0^2(\Gamma)$ of this problem we have $(\tilde{\mathbf{u}}, \tilde{p}) = (\mathbf{u}_T^*, p^*)$.*

The property $(\tilde{\mathbf{u}}, \tilde{p}) = (\mathbf{u}_T^*, p^*)$ explains, why we call this a *consistent* penalty formulation.

An *inconsistent* penalty surface Stokes formulation is: Determine $(\mathbf{u}, p) \in \mathbf{V}_* \times L_0^2(\Gamma)$ such that

$$\begin{aligned} A(\mathbf{u}, \mathbf{v}) + b_T(\mathbf{v}, p) &= (\mathbf{f}, \mathbf{v})_{L^2(\Gamma)} \quad \text{for all } \mathbf{v} \in \mathbf{V}_*, \\ b_T(\mathbf{u}, q) &= -(g, q)_{L^2(\Gamma)} \quad \text{for all } q \in L^2(\Gamma). \end{aligned} \quad (\text{P2})$$

From Theorem 3.1 in [25] we get the following result:

LEMMA 3.2. *Assume η is sufficiently large. Then the problem (P2) is well-posed and for the unique solution $(\hat{\mathbf{u}}, \hat{p}) \in \mathbf{V}_* \times L_0^2(\Gamma)$ we have:*

$$\|\hat{\mathbf{u}}_T - \mathbf{u}_T^*\|_{H^1(\Gamma)} + \|\hat{u}_N\|_{L^2(\Gamma)} + \|\hat{p} - p^*\|_{L^2(\Gamma)} \leq C\eta^{-1}(\|\mathbf{f}\|_{L^2(\Gamma)} + \|g\|_{L^2(\Gamma)}).$$

The unique velocity solution $\hat{\mathbf{u}}$ of (P2) has a normal component that in general is nonzero. Due to $\|\hat{u}_N\|_{L^2(\Gamma)} \leq C\eta^{-1}(\|\mathbf{f}\|_{L^2(\Gamma)} + \|g\|_{L^2(\Gamma)})$ its size can be controlled by the penalty parameter η .

4. Parametric finite element space for high order surface approximation. Clearly, for a higher order accurate finite element discretization of the variational problems (P1) and (P2) one needs a sufficiently accurate approximation of the surface Γ . For this we use the *parametric* trace finite element approach as in [11, 15]. In this section we outline the parametric mapping and the corresponding finite element space used in this method and summarize certain properties, known from the literature.

Let $\{\mathcal{T}_h\}_{h>0}$ be a family of shape regular tetrahedral triangulations of Ω . By V_h^k we denote the standard finite element space of continuous piecewise polynomials of degree k . The nodal interpolation operator in V_h^k is denoted by I^k . As input for the parametric mapping we need an approximation of ϕ . We consider geometry approximations whose order of approximation may differ from the order of the polynomials used in the finite element space (introduced below). In other words, the spaces that we consider are not necessarily *isoparametric*. Let k_g be the geometry approximation order, i.e., the construction of the geometry approximation will be based on a level set function approximation $\phi_h \in V_h^{k_g}$. We assume that for this approximation the error estimate

$$\max_{T \in \mathcal{T}_h} |\phi_h - \phi|_{W^{l,\infty}(T \cap U_\delta)} \leq ch^{k_g+1-l}, \quad 0 \leq l \leq k_g + 1, \quad (4.1)$$

is satisfied. Here, $|\cdot|_{W^{l,\infty}(T \cap U_\delta)}$ denotes the usual semi-norm on the Sobolev space $W^{l,\infty}(T \cap U_\delta)$ and the constant c depends on ϕ but is independent of h . The zero level set of the finite element function ϕ_h *implicitly* characterizes an approximation of the interface, which, however, is hard to compute for $k_g \geq 2$. With the piecewise *linear* nodal interpolation of ϕ_h , which is denoted by $\hat{\phi}_h = I^1\phi_h$, we define the low order geometry approximation:

$$\Gamma^{\text{lin}} := \{x \in \Omega \mid \hat{\phi}_h(x) = 0\},$$

which can easily be determined. The tetrahedra $T \in \mathcal{T}_h$ that have a nonzero intersection with Γ^{lin} are collected in the set denoted by \mathcal{T}_h^Γ . The domain formed by all tetrahedra in \mathcal{T}_h^Γ is denoted by $\Omega_h^\Gamma := \{x \in T \mid T \in \mathcal{T}_h^\Gamma\}$. Let $\Theta_h^{k_g} \in (V_h^{k_g}|_{\Omega_h^\Gamma})^3$ be the mesh transformation of order k_g as defined in [11], cf. Remark 4.1.

REMARK 4.1. We outline the key idea of the mesh transformation $\Theta_h^{k_g}$. For a detailed description and analysis we refer to [11, 19, 20]. There exists a unique $\tilde{d}: \Omega_h^\Gamma \rightarrow \mathbb{R}$ such that $\tilde{d}(x)$ is the in absolute value smallest number such that

$$\phi(x + \tilde{d}(x)\nabla\phi(x)) = \hat{\phi}_h(x) \quad \text{for } x \in \Omega_h^\Gamma.$$

Using \tilde{d} we define the injective mapping

$$\Psi(x) := x + \tilde{d}(x)\nabla\phi(x), \quad x \in \Omega_h^\Gamma,$$

which has the property $\Psi(\Gamma^{\text{lin}}) = \Gamma$. This mapping Ψ deforms the mesh \mathcal{T}_h^Γ in such a way that the (available) surface approximation Γ^{lin} is mapped to the exact surface Γ . To avoid computations with ϕ (which even may not be available) we use a similar construction with ϕ replaced by its (finite element) approximation ϕ_h . The resulting mapping Ψ_h is not necessarily a finite element function. The mesh transformation $\Theta_h^{k_g}$ is obtained by a simple projection (based on local averaging of values around a vertex) of Ψ_h into the finite element space $(V_h^{k_g}|_{\Omega_h^\Gamma})^3$. This parametric mapping is easy to determine. Implementation aspects are discussed in [19]. The mapping is implemented in Netgen/NGSolve [1].

An approximation of Γ is defined by

$$\Gamma_h^{k_g} := \Theta_h^{k_g}(\Gamma^{\text{lin}}) = \left\{x \mid \hat{\phi}_h((\Theta_h^{k_g})^{-1}(x)) = 0\right\}.$$

In [20] it is shown that (under certain reasonable smoothness assumptions) the estimate

$$\text{dist}(\Gamma_h^{k_g}, \Gamma) \lesssim h^{k_g+1} \quad (4.2)$$

holds. Here and further in the paper we write $x \lesssim y$ to state that there exists a constant $c > 0$, which is independent of the mesh parameter h and the position of Γ in the background mesh, such that the inequality $x \leq cy$ holds. Hence, the parametric mapping $\Theta_h^{k_g}$ indeed yields a higher order surface approximation. We denote the transformed cut mesh domain by $\Omega_\Theta^\Gamma := \Theta_h^{k_g}(\Omega_h^\Gamma)$ and apply to V_h^k the transformation $\Theta_h^{k_g}$ resulting in the *parametric spaces* (defined on Ω_Θ^Γ)

$$V_{h,\Theta}^{k,k_g} := \left\{ v_h \circ (\Theta_h^{k_g})^{-1} \mid v_h \in V_h^k|_{\Omega_h^\Gamma} \right\}, \quad \mathbf{V}_{h,\Theta}^{k,k_g} := (V_{h,\Theta}^{k,k_g})^3.$$

Note that k_g denotes the degree of the polynomials used in the parametric mapping $\Theta_h^{k_g}$, which determines the accuracy of the geometry approximation, cf. (4.2), and k the degree of the polynomials used in the finite element space. To simplify the notation we delete the superscript k_g and write

$$V_{h,\Theta}^k = V_{h,\Theta}^{k,k_g}, \quad \mathbf{V}_{h,\Theta}^k = \mathbf{V}_{h,\Theta}^{k,k_g}, \quad \Theta_h = \Theta_h^{k_g}, \quad \Gamma_h = \Gamma_h^{k_g}.$$

The following lemma, taken from [11], gives an approximation error for the easy to compute normal approximation \mathbf{n}_h , which is used in the methods introduced below.

LEMMA 4.1. *For $x \in T \in \mathcal{T}_h^\Gamma$ define*

$$\mathbf{n}_{lin} = \mathbf{n}_{lin}(T) := \frac{\nabla \hat{\phi}_h(x)}{\|\nabla \hat{\phi}_h(x)\|_2} = \frac{\nabla \hat{\phi}_h|_T}{\|\nabla \hat{\phi}_h|_T\|_2}, \quad \mathbf{n}_h(\Theta(x)) := \frac{D\Theta_h(x)^{-T} \mathbf{n}_{lin}}{\|D\Theta_h(x)^{-T} \mathbf{n}_{lin}\|_2}.$$

Let $\mathbf{n}_{\Gamma_h}(x)$, $x \in \Gamma_h$ a.e., be the unit normal on Γ_h (in the direction of $\phi_h > 0$). The following holds:

$$\begin{aligned} \|\mathbf{n}_h - \mathbf{n}\|_{L^\infty(\Omega_\Theta^\Gamma)} &\lesssim h^{k_g}, \\ \|\mathbf{n}_{\Gamma_h} - \mathbf{n}\|_{L^\infty(\Gamma_h)} &\lesssim h^{k_g}. \end{aligned}$$

5. Higher order trace finite element methods. In this section we introduce a class of higher order parametric trace finite element methods. These methods are obtained by applying a Galerkin approach (modulo a geometry error due to $\Gamma_h \approx \Gamma$) to the formulations (P1) and (P2). Based on the parametric finite element spaces $\mathbf{V}_{h,\Theta}^k$ and $V_{h,\Theta}^k$ we introduce for $k \geq 2$ the \mathbf{P}_k - P_{k-1} pair of *parametric trace Taylor-Hood elements*:

$$\mathbf{U}_h := \mathbf{V}_{h,\Theta}^k, \quad Q_h := V_{h,\Theta}^{k-1} \cap L_0^2(\Gamma_h).$$

Note that the polynomial degrees, k and $k-1$, for the velocity and pressure approximation are different, but both spaces \mathbf{U}_h and Q_h use the same parametric mapping based on polynomials of degree k_g . Since the pressure approximation uses H^1 finite element functions we can use the partial integration (2.5) (with Γ replaced by Γ_h).

We introduce discrete variants of the bilinear forms $a(\cdot, \cdot)$, $a_T(\cdot, \cdot)$, $b_T(\cdot, \cdot)$ and the penalty bilinear form $k(\cdot, \cdot)$ introduced above. Since we use a trace FEM, we need a stabilization that eliminates instabilities caused by the small cuts. For this we use the so-called “normal derivative volume stabilization”, known from the literature [6, 11] ($s_h(\cdot, \cdot)$ and $\tilde{s}_h(\cdot, \cdot)$ below). We define, with $\mathbf{P}_h = \mathbf{P}_h(x) := \mathbf{I} - \mathbf{n}_h(x)\mathbf{n}_h(x)^T$, $x \in \Omega_\Theta^\Gamma$:

$$\begin{aligned} \nabla_{\Gamma_h} \mathbf{u} &:= \mathbf{P}_h \nabla \mathbf{u} \mathbf{P}_h, \\ E_h(\mathbf{u}) &:= \frac{1}{2} (\nabla_{\Gamma_h} \mathbf{u} + \nabla_{\Gamma_h}^T \mathbf{u}), \quad E_{T,h}(\mathbf{u}) := E_h(\mathbf{u}) - u_N \mathbf{H}_h, \\ a_h(\mathbf{u}, \mathbf{v}) &:= \int_{\Gamma_h} E_h(\mathbf{u}) : E_h(\mathbf{v}) ds_h + \int_{\Gamma_h} \mathbf{u} \cdot \mathbf{v} ds_h, \\ a_{T,h}(\mathbf{u}, \mathbf{v}) &:= \int_{\Gamma_h} E_{T,h}(\mathbf{u}) : E_{T,h}(\mathbf{v}) ds_h + \int_{\Gamma_h} \mathbf{P}_h \mathbf{u} \cdot \mathbf{P}_h \mathbf{v} ds_h, \\ b_h(\mathbf{u}, q) &:= \int_{\Gamma_h} \mathbf{u} \cdot \nabla_{\Gamma_h} q ds_h, \\ k_h(\mathbf{u}, \mathbf{v}) &:= \eta \int_{\Gamma_h} (\mathbf{u} \cdot \tilde{\mathbf{n}}_h)(\mathbf{v} \cdot \tilde{\mathbf{n}}_h) ds_h, \\ s_h(\mathbf{u}, \mathbf{v}) &:= \rho_u \int_{\Omega_\Theta^\Gamma} (\nabla \mathbf{u} \mathbf{n}_h) \cdot (\nabla \mathbf{v} \mathbf{n}_h) dx, \quad \tilde{s}_h(p, q) := \rho_p \int_{\Omega_\Theta^\Gamma} (\mathbf{n}_h \cdot \nabla p)(\mathbf{n}_h \cdot \nabla q) dx. \end{aligned}$$

The normal vector $\tilde{\mathbf{n}}_h$, used in the penalty term $k_h(\cdot, \cdot)$, and the curvature tensor \mathbf{H}_h are approximations of the exact normal and the exact Weingarten mapping, respectively. The reason that we introduce yet another normal approximation $\tilde{\mathbf{n}}_h$ is the following. From an error analysis of the vector-Laplace problem in [13, 15], cf. also section 6 below, it follows that for obtaining optimal order estimates the normal approximation $\tilde{\mathbf{n}}_h$ used in the penalty term has to be more accurate than the normal approximation \mathbf{n}_h . How suitable approximations $\tilde{\mathbf{n}}_h$ and \mathbf{H}_h can be determined is discussed in Section 6. Suitable choices of the stabilization parameters ρ_u , ρ_p and the penalty parameter η are also discussed in Section 6. As a discrete analogon of $E(\mathbf{u}_T) = E(\mathbf{P}\mathbf{u}) = E(\mathbf{u}) - u_N \mathbf{H}$ we use $E_{T,h}(\mathbf{u}) = E_h(\mathbf{u}) - u_N \mathbf{H}_h$ instead of $E_{T,h}(\mathbf{u}) = E_h(\mathbf{P}_h \mathbf{u})$, because the latter requires (tangential) differentiation of \mathbf{P}_h , which causes difficulties. The (canonical) choice of \mathbf{n}_h as in Lemma 4.1 is discontinuous across faces, hence *not* an $H^1(\Gamma_h)$ vector function, which implies that $E_h(\mathbf{P}_h \mathbf{u})$ is in general not well-defined.

We now introduce discrete versions of the formulations (P1) and (P2). For these we need a suitable (sufficiently accurate) extension of the data \mathbf{f} and g to Γ_h , which are denoted by \mathbf{f}_h and g_h , respectively.

Consistent discrete surface Stokes. This method is based on the *consistent* formulation (P1) and uses the bilinear form $a_{T,h}(\cdot, \cdot)$. Define

$$A_{T,h}(\mathbf{u}, \mathbf{v}) := a_{T,h}(\mathbf{u}, \mathbf{v}) + s_h(\mathbf{u}, \mathbf{v}) + k_h(\mathbf{u}, \mathbf{v}).$$

The discrete problem reads: determine $(\mathbf{u}_h, p_h) \in \mathbf{U}_h \times Q_h$ such that

$$\begin{aligned} A_{T,h}(\mathbf{u}_h, \mathbf{v}_h) + b_h(\mathbf{v}_h, p_h) &= (\mathbf{f}_h, \mathbf{v}_h)_{L^2(\Gamma_h)} & \text{for all } \mathbf{v}_h \in \mathbf{U}_h \\ b_h(\mathbf{u}_h, q_h) - \tilde{s}_h(p_h, q_h) &= (-g_h, q_h)_{L^2(\Gamma_h)} & \text{for all } q_h \in Q_h. \end{aligned} \tag{P1h}$$

Note that, although we call this method “consistent”, due to geometry errors it does contain consistency errors.

Inconsistent discrete surface Stokes. This method is based on the *inconsistent* formulation (P2) and uses the bilinear form $a_h(\cdot, \cdot)$. Define

$$A_h(\mathbf{u}, \mathbf{v}) := a_h(\mathbf{u}, \mathbf{v}) + s_h(\mathbf{u}, \mathbf{v}) + k_h(\mathbf{u}, \mathbf{v}).$$

The discrete problem reads: determine $(\mathbf{u}_h, p_h) \in \mathbf{U}_h \times Q_h$ such that

$$\begin{aligned} A_h(\mathbf{u}_h, \mathbf{v}_h) + b_h(\mathbf{v}_h, p_h) &= (\mathbf{f}_h, \mathbf{v}_h)_{L^2(\Gamma_h)} && \text{for all } \mathbf{v}_h \in \mathbf{U}_h \\ b_h(\mathbf{u}_h, q_h) - \tilde{s}_h(p_h, q_h) &= (-g_h, q_h)_{L^2(\Gamma_h)} && \text{for all } q_h \in Q_h. \end{aligned} \quad (\text{P2h})$$

In the next section we explain how components of these methods, for example the penalty parameter η and the Weingarten mapping approximation \mathbf{H}_h , can be chosen. In Section 7 we present numerical results for these methods.

6. Choice of method components based on available analysis. Before the finite element discretizations (P1h) and (P2h) can be applied to a specific surface Stokes problem, the following issues have to be addressed:

- a) Accuracy of geometry approximation: given k , how should one take k_g ?
- b) Components in penalty term: how does η depend on h , how to choose $\tilde{\mathbf{n}}_h$?
- c) Parameters in volume normal derivative stabilizations: how do ρ_u, ρ_p depend on h ?
- d) Weingarten mapping approximation (only for consistent method): what is a suitable choice for \mathbf{H}_h ?

In this section we address these issues and give specific recommendations. These are based on recent analyses of surface vector-Laplace and surface Stokes equations. Below we first summarize a few relevant results of these analyses that will be used to answer the questions above. It is convenient to introduce one further order parameter $k_p \geq k$ (besides k and k_g) that describes the accuracy of the normal approximation $\tilde{\mathbf{n}}_h$:

$$\|\mathbf{n} - \tilde{\mathbf{n}}_h\|_{L^\infty(\Gamma_h)} \lesssim h^{k_p}. \quad (6.1)$$

In [15] discrete vector-Laplace problems are studied that can be seen as simplifications of the problems (P1h) and (P2h). More precisely, in the vector-Laplace equation, the only unknown is a tangential velocity field \mathbf{u} (no pressure) that has to satisfy the equation $-\mathbf{P} \operatorname{div}_\Gamma(E(\mathbf{u})) + \mathbf{u} = \mathbf{f}$ on Γ , which is similar to (2.1). The same parametric finite element techniques as described above are applied and yield discrete problems as in the first equations in (P1h) and (P2h), with $b_h(\cdot, \cdot)$ put to zero. For these discretizations a complete error analysis (including geometry errors) is presented in [15]. In that analysis the natural energy norm $\|\cdot\|_A$, defined by $\|\mathbf{v}\|_A^2 = \|\mathbf{v}\|_{A_{\Gamma,h}}^2$ for the consistent method and $\|\mathbf{v}\|_A^2 = \|\mathbf{v}\|_{A_h}^2$ for the inconsistent one, is used. Main results of the error analysis are the following (we refer to citejankuhn2019 for precise formulations of these results):

- For the consistent method. Assume $\|\mathbf{H} - \mathbf{H}_h\|_{L^\infty(\Gamma_h)} \lesssim h^{k_g-1}$, $k_g = k$ (isoparametric case), $\eta \sim h^{-2}$, $k_p = k + 1$, $\rho_u \sim h^{-1}$, $\rho_p \sim h$. Then an

optimal order error bound of order $\mathcal{O}(h^k)$ in the energy norm holds. This bound implies an optimal error bound in the $H^1(\Gamma_h)$ -norm of the same order.

- For the inconsistent method. Assume $k_g = k$ (isoparametric case), $\eta \sim h^{-(k+1)}$, $k_p = k + 1$, $\rho_u \sim h^{-1}$, $\rho_p \sim h$. Then an optimal order error bound of order $\mathcal{O}(h^{\frac{1}{2}(k+1)})$ in the energy norm holds. This bound implies an error bound in the $H^1(\Gamma_h)$ -norm of the same order, which is optimal only for the case $k = 1$.

Furthermore, numerical experiments indicate the following:

- The inconsistent method, with parameters as above, has optimal order $\mathcal{O}(h^k)$ -convergence in the $H^1(\Gamma_h)$ -norm and optimal order $\mathcal{O}(h^{k+1})$ -convergence in the $L^2(\Gamma_h)$ -norm not only for $k = 1$ but also for $k \geq 2$.
- Taking $k_p = k$ leads to suboptimal convergence behavior for both the consistent and the inconsistent method.
- For the inconsistent method and $k \geq 2$, optimal order convergence is lost if for the penalty parameter we use a scaling $\eta \sim h^{-2}$.

For these results to hold, one needs a sufficiently accurate data extension \mathbf{f}_h of \mathbf{f} . Precise conditions are given in [15] and are very similar to the conditions formulated for higher order methods for *scalar* surface PDEs [7, 29].

In the recent paper [27] the discretizations (P1h) and (P2h) are studied for the case *without geometry errors*, i.e., $\Gamma_h = \Gamma$. In that case we do not need the parametric mapping Θ_h and the finite element spaces are simply the Taylor-Hood pairs on the local triangulation, consisting of the tetrahedra intersected by Γ . Clearly, this method is in general not feasible in practice, because integrals over Γ can not be evaluated efficiently. This (simplified) setting, however, is used to analyze the discrete inf-sup stability of the trace Taylor-Hood pair for the surface Stokes problem. A main result derived in [27] is the following (we refer to [27] for precise formulation):

- Assume $h \lesssim \rho_u \lesssim h^{-1}$, $\rho_p \sim h$, $\eta \sim h^{-2}$. Then both for the consistent and inconsistent variant the discrete inf-sup stability estimate

$$\|q\|_{L^2(\Gamma)} \lesssim \sup_{\mathbf{v} \in \mathbf{U}_h} \frac{b_T(\mathbf{v}, q)}{\|\mathbf{v}\|_A} + \tilde{s}_h(q, q)^{\frac{1}{2}} \quad \text{for all } q \in Q_h, \quad (6.2)$$

holds for $k = 2$, i.e., for the \mathbf{P}_2 - P_1 trace Taylor-Hood pair.

- For this parameter choice of ρ_u , ρ_p and η the consistent method has an optimal error bound (in $H^1(\Gamma)$ -norm for velocity and $L^2(\Gamma)$ -norm for pressure).

Based on these results, for the discretizations (P1h) and (P2h) of the surface Stokes problem we have the following recommendations concerning the issues a)-d) raised above.

a) *Accuracy of geometry approximation.* We take $k_g = k$, i.e. isoparametric finite elements for velocity.

b) *Components in penalty term.* For the consistent method we take $\eta \sim h^{-2}$ and for the inconsistent method $\eta \sim h^{-(k+1)}$. In both methods we use a normal approximation $\tilde{\mathbf{n}}_h$ with accuracy $k_p = k + 1$. Such an approximation can be determined as follows. We assume that we have an approximation $\tilde{\phi}_h$ of ϕ available that is one order more accurate than ϕ_h , i.e., it satisfies an error bound as in (4.1) with k_g replaced by

$k_g + 1$. We then take $\tilde{\mathbf{n}}_h := \frac{\nabla \tilde{\phi}_h}{\|\nabla \tilde{\phi}_h\|}$.

c) *Parameters in volume normal derivative stabilizations.* We take $\rho_u \sim h^{-1}$, $\rho_p \sim h$.

d) *Weingarten mapping approximation* (only for consistent method). We use an approximation \mathbf{H}_h with order of accuracy $k_g - 1$. Such an approximation can be obtained by taking $\mathbf{H}_h = \nabla(I_{\Theta}^{k_g}(\mathbf{n}_h))$, where $I_{\Theta}^{k_g}$ denotes the (componentwise) parametric nodal interpolation in the space $V_{h,\Theta}^{k_g}$, cf. [11].

7. Numerical experiments. In this section we present results of numerical experiments. As test cases we consider Stokes equations on a sphere and a torus. For these two cases we first describe the setting of the continuous problem.

The unit sphere Γ is characterized by the zero level of the distance function $\phi(x) = \sqrt{x_1^2 + x_2^2 + x_3^2} - 1$, $x = (x_1, x_2, x_3)^T$. The surface is embedded in the domain $\Omega = [-5/3, 5/3]^3$. We consider the surface Stokes problem (2.6) with the prescribed solution

$$\mathbf{u}(x) = \begin{pmatrix} \frac{(x_2^2 x_3^2 + x_3^4) \sqrt{x_1^2 + x_2^2 + x_3^2} + x_1 (x_1^2 + x_2^2 + x_3^2) (x_1 x_3 + x_2^2)}{(x_1^2 + x_2^2 + x_3^2)^{\frac{3}{2}}} \\ \frac{x_1 x_3^2 \sqrt{x_1^2 + x_2^2 + x_3^2} + (x_1^2 - x_1 x_3 + x_3^2) (x_1^2 + x_2^2 + x_3^2) x_2}{(x_1^2 + x_2^2 + x_3^2)^{\frac{3}{2}}} \\ \frac{x_1 x_3^3 \sqrt{x_1^2 + x_2^2 + x_3^2} + (x_1^2 + x_2^2 + x_3^2) (x_1^3 + x_1 x_2^2 - x_2^2 x_3)}{(x_1^2 + x_2^2 + x_3^2)^{\frac{3}{2}}} \end{pmatrix},$$

$$p(x) = \frac{x_1 x_2^3 + x_3 (x_1^2 + x_2^2 + x_3^2)^{\frac{3}{2}}}{(x_1^2 + x_2^2 + x_3^2)^2}.$$

The velocity solution is tangential, i.e. $\mathbf{P}\mathbf{u} = \mathbf{u}$ and constant in normal direction, i.e., $\mathbf{u} = \mathbf{u}^e$. The velocity field \mathbf{u} is not divergence-free, i.e., $\text{div}_{\Gamma} \mathbf{u} \neq 0$. The pressure solution is also constant in normal direction, i.e. $p = p^e$ as well as mean free, i.e. $\int_{\Gamma} p \, ds = 0$. Corresponding right-hand sides \mathbf{f} and g are computed in a small neighborhood of Γ as follows. The surface differential operators used in the Stokes problem (2.1), defined on Γ , have canonical extensions to a small neighborhood of Γ . We use these extended ones and apply the Stokes operator (defined in the neighborhood) to the prescribed \mathbf{u} and p , which are constant in normal direction. The resulting \mathbf{f} and g , which are defined in the neighborhood and not necessarily constant in normal direction, are used as data \mathbf{f}_h and g_h in the finite element method.

For the case of a torus, Γ is characterized by the zero level of the distance function $\phi(x) = \sqrt{x_3^2 + (\sqrt{x_1^2 + x_2^2} - 1)^2} - \frac{1}{2}$. The surface is again embedded in the domain $\Omega = [-5/3, 5/3]^3$. We consider the surface Stokes problem (2.6) with the prescribed solution

$$\mathbf{u}(x) = \mathbf{v}^e(x) \quad \text{with} \quad \mathbf{v}(x) = \begin{pmatrix} \frac{x_3^2 x_1}{(x_1^2 + x_2^2 + x_3^2 - 2\sqrt{x_1^2 + x_2^2} + 1)\sqrt{x_1^2 + x_2^2}} \\ \frac{x_2 x_3^2}{(x_1^2 + x_2^2 + x_3^2 - 2\sqrt{x_1^2 + x_2^2} + 1)\sqrt{x_1^2 + x_2^2}} \\ -\frac{(\sqrt{x_1^2 + x_2^2} - 1)x_3}{x_1^2 + x_2^2 + x_3^2 - 2\sqrt{x_1^2 + x_2^2} + 1} \end{pmatrix},$$

$$p(x) = q^e(x) - \frac{\int_{\Gamma} q^e \, ds}{\int_{\Gamma} 1 \, ds} \quad \text{with} \quad q(x) = x_1 x_2^3 + x_3.$$

The velocity solution is tangential, i.e. $\mathbf{P}\mathbf{u} = \mathbf{u}$ and constant in normal direction, i.e. $\mathbf{u} = \mathbf{u}^e$. The velocity field \mathbf{u} is not divergence-free, i.e., $\text{div}_\Gamma \mathbf{u} \neq 0$. The pressure solution is also constant in normal direction, i.e., $p = p^e$. The right-hand sides \mathbf{f}_h and g_h for the finite element discretization are computed in the same way as for the sphere above.

In both cases, for the construction of the local triangulation \mathcal{T}_h^Γ we start with an unstructured tetrahedral Netgen-mesh with $h_{max} = 0.5$ (see [33]) and locally refine the mesh using a marked-edge bisection method (refinement of tetrahedra that are intersected by the surface).

In the implementation of the discretizations (P1h) and (P2h) of the surface Stokes problem, we use (unless stated otherwise) the parameter setting and components listed in a)-d) at the end of section 6 (with a constant 1 in \sim). The methods are implemented in Netgen/NGSolve with ngsxfem [1, 18].

The errors are measured in different (semi-)norms. We use the following notations:

$$\begin{aligned} e_{L^2}^{\mathbf{u}} &:= \|\mathbf{u} - \mathbf{u}_h\|_{L^2(\Gamma_h)}, & e_{H^1}^{\mathbf{u}} &:= \|\nabla_{\Gamma_h}(\mathbf{u} - \mathbf{u}_h)\|_{L^2(\Gamma_h)}, & e_M^p &:= \|p - p_h\|_M, \\ e_{PL^2}^{\mathbf{u}} &:= \|\mathbf{P}_h(\mathbf{u} - \mathbf{u}_h)\|_{L^2(\Gamma_h)}, & e_A^{\mathbf{u}} &:= \|\mathbf{u} - \mathbf{u}_h\|_A. \end{aligned}$$

Here $\|\cdot\|_M^2 := \|\cdot\|_{L^2(\Gamma_h)}^2 + \tilde{s}_h(\cdot, \cdot)$.

7.1. Results for the sphere. In Section 7.1.1 we present results of numerical experiments that show optimal convergence orders for \mathbf{P}_2 - P_1 and \mathbf{P}_3 - P_2 finite elements and comment on the choice of the stabilization parameters ρ_u and ρ_p . We also compare the consistent and inconsistent methods. In Section 7.1.2 we discuss the choice of the parameters in the penalty term and the effects the penalty term has on the energy norm error.

7.1.1. Optimal results for \mathbf{P}_2 - P_1 and \mathbf{P}_3 - P_2 finite elements. We begin with the consistent formulation (P1h). In Figure 7.1 we show the errors for \mathbf{P}_2 - P_1 and \mathbf{P}_3 - P_2 finite elements. We clearly observe optimal orders of convergence: $e_A^{\mathbf{u}} \sim h^k$, $e_{H^1}^{\mathbf{u}} \sim h^k$, $e_M^p \sim h^k$ and $e_{L^2}^{\mathbf{u}} \sim h^{k+1}$, $e_{PL^2}^{\mathbf{u}} \sim h^{k+1}$.

Concerning the choice of the stabilization parameters ρ_u and ρ_p we note the following (results of the experiments are not shown). For \mathbf{P}_2 - P_1 finite elements and $\rho_u = h$, instead of $\rho_u = h^{-1}$, (and other parameters the same as above) we observe slightly slower than $\mathcal{O}(h^2)$ -convergence for the energy norm error $e_A^{\mathbf{u}}$ and less than $\mathcal{O}(h^3)$ -convergence for the L^2 -error $e_{L^2}^{\mathbf{u}}$. These suboptimal convergence orders are probably due to the consistency error (geometry error), since taking superparametric finite elements, i.e. $k_g = 3$, leads to optimal convergence orders. If we take $\rho_p = h^{-1}$ instead of h (and other parameters the same as above), we observe a loss of one order in the errors $e_A^{\mathbf{u}}$ and e_M^p and even a loss of one and a half order in $e_{L^2}^{\mathbf{u}}$. Taking $\rho_p = 1$ results in a loss of a half order for e_M^p , a loss of a quarter order for $e_{L^2}^{\mathbf{u}}$ and a loss of a half order for $e_{PL^2}^{\mathbf{u}}$.

We now consider the inconsistent formulation (P2h). In Figure 7.2 we show the errors for \mathbf{P}_2 - P_1 and \mathbf{P}_3 - P_2 finite elements. We observe $\mathcal{O}(h^{\frac{1}{2}(k+1)})$ -convergence for the energy norm error $e_A^{\mathbf{u}}$, which is what we expect to see based on the analysis in [15]. For the $e_{H^1}^{\mathbf{u}}$ - and e_M^p -errors we have $\mathcal{O}(h^k)$ -convergence and for the L^2 -errors $e_{L^2}^{\mathbf{u}}$ and $e_{PL^2}^{\mathbf{u}}$ we see $\mathcal{O}(h^{k+1})$ -convergence, which are all optimal.

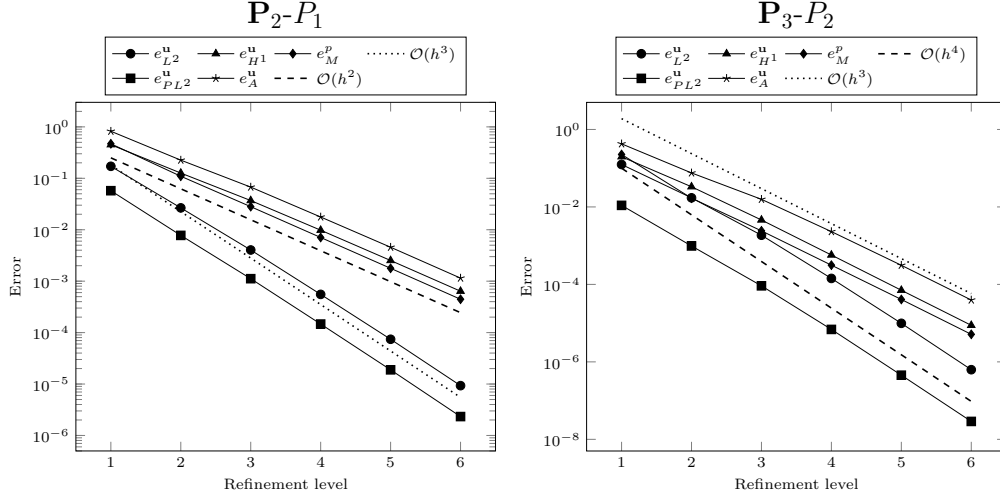


Fig. 7.1: Consistent formulation (P1h) on the unit sphere

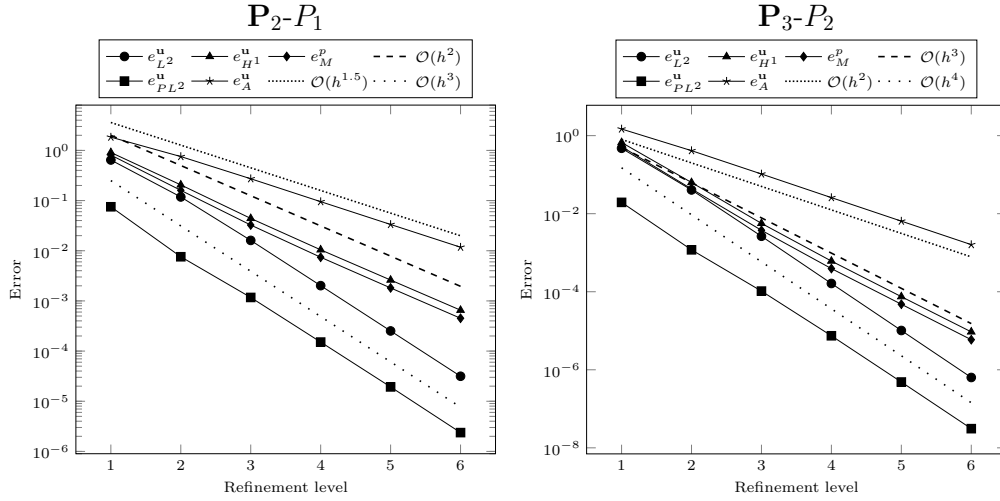


Fig. 7.2: Inconsistent formulation (P2h) on the unit sphere

A different scaling of the stabilization parameter ρ_u does not have the same effect on the convergence behavior as described above for the consistent method (P1h). For P_2 - P_1 finite elements and $\rho_u = h$ we still observe the same optimal convergence order as for $\rho_u = h^{-1}$. For the stabilization parameter ρ_p , however, we see similar effects as described above for the consistent formulation (P1h).

Both methods (P1h) and (P2h) have optimal order errors $e_{L^2}^u$ and $e_{H^1}^u$. The question arises which of the two methods results in a smaller absolute error. Therefore,

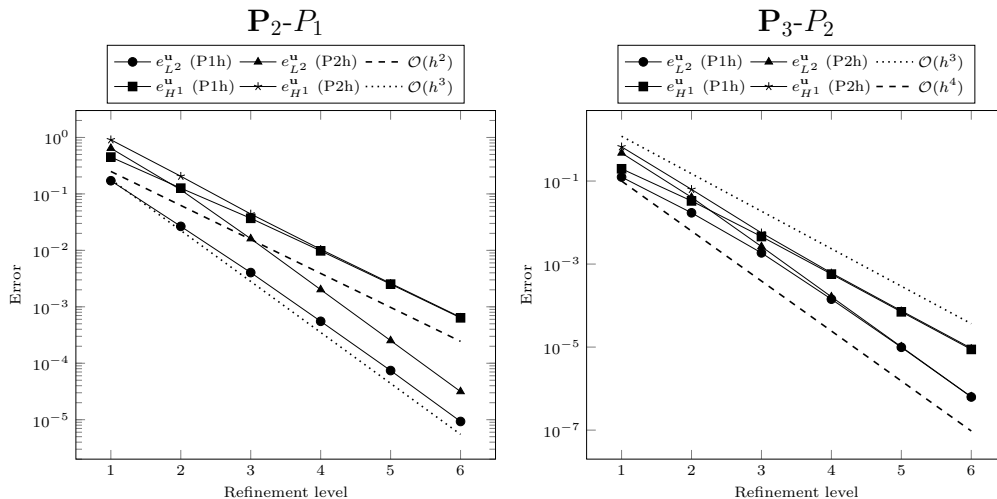


Fig. 7.3: Comparison of (P1h) and (P2h) on the unit sphere

in Figure 7.3 we show the $e_{L^2}^{\mathbf{u}}$ - and $e_{H^1}^{\mathbf{u}}$ -errors for both methods in one plot. For \mathbf{P}_2 - P_1 finite elements the $e_{H^1}^{\mathbf{u}}$ -errors differ only slightly for the first three refinement levels and the $e_{L^2}^{\mathbf{u}}$ -error of the consistent formulation is approximately one order of magnitude smaller than the one of the inconsistent formulation. For \mathbf{P}_3 - P_2 finite elements the errors of both methods are almost the same.

REMARK 7.1. A special situation occurs if one considers a Stokes problem on the sphere with a divergence-free velocity solution \mathbf{u} . In such a case the energy norm of the inconsistent method is not of order $e_A^{\mathbf{u}} \sim h^{\frac{1}{2}(k+1)}$ (as in the results above), but of order $e_A^{\mathbf{u}} \sim h^k$. This improvement can be explained as follows. From the analysis in [15] we notice that for the inconsistent method the dominant inconsistency term is

$$(E(\mathbf{u}), (\mathbf{v}_h^l \cdot \mathbf{n})\mathbf{H})_{L^2(\Gamma)} = \int_{\Gamma} (\mathbf{v}_h^l \cdot \mathbf{n}) \text{tr}(E(\mathbf{u})\mathbf{H}) \, ds,$$

with \mathbf{v}_h^l the lifting of a finite element function from Γ_h to Γ . For the sphere we have $\mathbf{H} = \mathbf{P}$ and thus

$$\text{tr}(E(\mathbf{u})\mathbf{H}) = \text{div}_{\Gamma}(\mathbf{u}),$$

which vanishes for a divergence-free solution \mathbf{u} .

7.1.2. Effects related to the penalty term. As mentioned in Section 6, in case of the vector-Laplace problem, for optimal convergence it is essential that one uses $k_p = k + 1$ (i.e. a one order better approximation for the normal approximation $\tilde{\mathbf{n}}_h$). For the Stokes problem we performed an experiment with \mathbf{P}_2 - P_1 finite elements in which all parameters and components are the same as in the experiments above, except for k_p : we take $k_p = 2$ instead of $k_p = 3$. The results are presented in Figure 7.4. In case of the consistent formulation (P1h) we lose, compared to $k_p = 3$, one

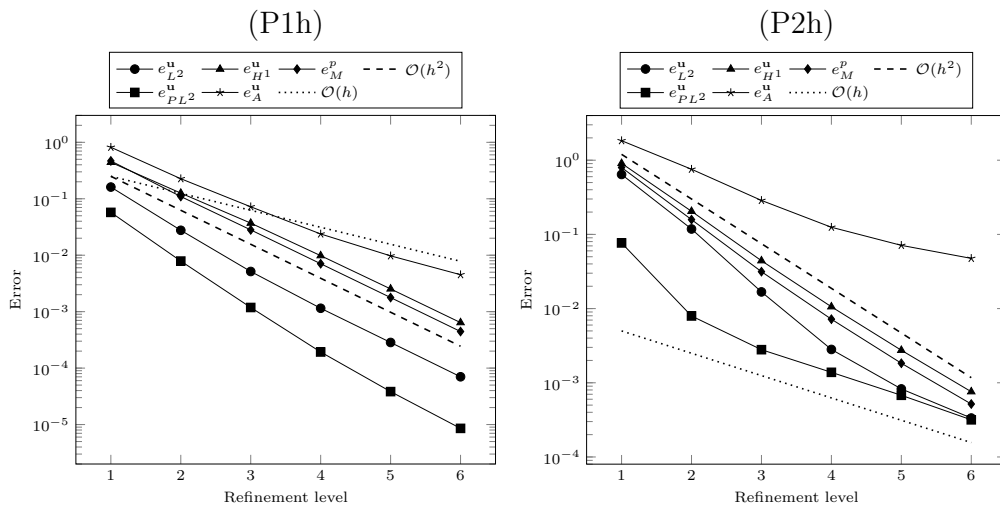


Fig. 7.4: \mathbf{P}_2 - P_1 finite elements with $k_p = 2$

order for the L^2 -errors $e_{L^2}^{\mathbf{u}}$ and $e_{PL^2}^{\mathbf{u}}$ and one order for the energy norm error $e_A^{\mathbf{u}}$. The convergence of the $e_{H^1}^{\mathbf{u}}$ -error and e_M^p -error is a little worse than $\mathcal{O}(h^2)$. For the inconsistent formulation (P2h) the effect is even stronger. In that case the L^2 -errors $e_{L^2}^{\mathbf{u}}$ and $e_{PL^2}^{\mathbf{u}}$ are only of order $\mathcal{O}(h)$ and the energy norm error $e_A^{\mathbf{u}}$ converges significantly slower than first order. The convergence of the $e_{H^1}^{\mathbf{u}}$ -error and e_M^p -error is a little worse than $\mathcal{O}(h^2)$.

As noted in Section 6, to obtain optimal convergence for the inconsistent formulation of the vector-Laplace problem the scaling of the penalty parameter η has to depend on the degree of the finite element space k : $\eta \sim h^{-(k+1)}$. For the inconsistent formulation of the Stokes problem (P2h) we performed an experiment with \mathbf{P}_2 - P_1 and \mathbf{P}_3 - P_2 finite elements in which all parameters and components are the same as in the experiments above, except for η : we take $\eta = h^{-2}$ instead of $\eta = h^{-(k+1)}$. The results are shown in Figure 7.5. For \mathbf{P}_2 - P_1 finite elements we observe suboptimal $\mathcal{O}(h)$ -convergence for the energy norm error $e_A^{\mathbf{u}}$, which is half an order less than for $\eta = h^{-3}$. We still have $\mathcal{O}(h^2)$ -convergence for the $e_{H^1}^{\mathbf{u}}$ - and e_M^p -errors and $\mathcal{O}(h^3)$ -convergence for the tangential L^2 -error $e_{PL^2}^{\mathbf{u}}$, which are both optimal. The full L^2 -error $e_{L^2}^{\mathbf{u}}$ though loses one order compared to $\eta = h^{-3}$. For \mathbf{P}_3 - P_2 finite elements we observe the same convergence orders for all the errors except for the tangential L^2 -error $e_{PL^2}^{\mathbf{u}}$, which is a bit better as for the \mathbf{P}_2 - P_1 case. Hence, for \mathbf{P}_3 - P_2 finite elements all errors show suboptimal convergence if we take $\eta = h^{-2}$.

Finally we briefly discuss the $\mathcal{O}(h^{\frac{1}{2}(k+1)})$ -convergence in the energy norm error $e_A^{\mathbf{u}}$ observed for the inconsistent method, cf. Figure 7.2. We call this convergence rate “optimal”, due to the penalty term which is included in the energy norm:

$$\|\mathbf{v}\|_A^2 = A_h(\mathbf{v}, \mathbf{v}) := a_h(\mathbf{v}, \mathbf{v}) + s_h(\mathbf{v}, \mathbf{v}) + k_h(\mathbf{v}, \mathbf{v}).$$

For all parameters and components we take the default values. For the penalty term

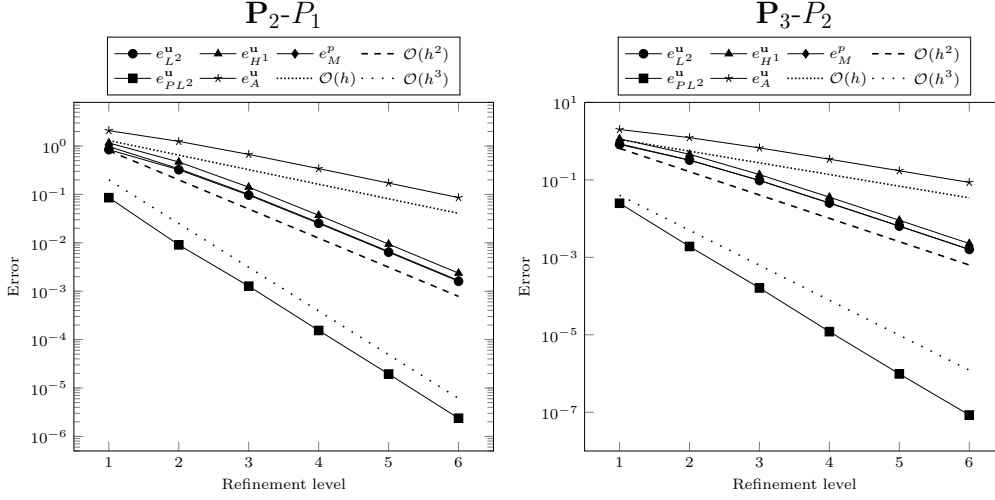


Fig. 7.5: Inconsistent formulation (P2h) with $\eta = h^{-2}$

part of the energy norm error $\|\mathbf{e}_h\|_A = e_A^u$ we have

$$k_h(\mathbf{e}_h, \mathbf{e}_h)^{\frac{1}{2}} = \eta^{\frac{1}{2}} \|\tilde{\mathbf{n}}_h \cdot \mathbf{e}_h\|_{L^2(\Gamma_h)} = h^{-\frac{1}{2}(k+1)} \|\tilde{\mathbf{n}}_h \cdot \mathbf{e}_h\|_{L^2(\Gamma_h)}.$$

For the term $\|\tilde{\mathbf{n}}_h \cdot \mathbf{e}_h\|_{L^2(\Gamma_h)}$ the best one can expect (based on an interpolation error) is $\|\tilde{\mathbf{n}}_h \cdot \mathbf{e}_h\|_{L^2(\Gamma_h)} \sim h^{k+1}$. Hence, for the penalty term part of the energy norm error we obtain an optimal convergence rate $k_h(\mathbf{e}_h, \mathbf{e}_h)^{\frac{1}{2}} \sim h^{\frac{1}{2}(k+1)}$. This explains why $h^{\frac{1}{2}(k+1)}$ is the ‘‘optimal’’ convergence rate for the energy norm error e_A^u , which is indeed attained for the inconsistent method and $k = 2$, $k = 3$, cf. Figure 7.2. To illustrate this, we performed an experiment in which the three different contributions to the energy norm error are shown separately. In Figure 7.6, for \mathbf{P}_2-P_1 and \mathbf{P}_3-P_2 finite elements, we show the energy norm $\|\mathbf{e}_h\|_A = e_A^u$ and its three components $a_h(\mathbf{e}_h, \mathbf{e}_h)^{\frac{1}{2}}$, $s_h(\mathbf{e}_h, \mathbf{e}_h)^{\frac{1}{2}}$, $k_h(\mathbf{e}_h, \mathbf{e}_h)^{\frac{1}{2}}$. We clearly observe that $e_A^u \approx k_h(\mathbf{e}_h, \mathbf{e}_h)^{\frac{1}{2}} \sim h^{\frac{1}{2}(k+1)}$. Furthermore, the other error components have a higher rate of convergence: $a_h(\mathbf{e}_h, \mathbf{e}_h)^{\frac{1}{2}} \sim h^k$ and $s_h(\mathbf{e}_h, \mathbf{e}_h)^{\frac{1}{2}} \sim h^k$.

7.2. Results for the torus. For the torus we performed experiments for the consistent and inconsistent method and with \mathbf{P}_2-P_1 and \mathbf{P}_3-P_2 finite elements. Again we used the default parameters. In Figure 7.7 we show the results for the consistent formulation (P1h) and in Figure 7.8 for the inconsistent formulation (P2h). The observed convergence rates are the same as for the sphere. For \mathbf{P}_3-P_2 finite elements we observe for both formulations a slight deterioration of the convergence rate for the tangential L^2 -error $e_{P_{L^2}}^u$ in the last refinement step. This may be due to a relatively large condition number of the stiffness matrix.

8. Conclusions and outlook. We proposed two trace finite element methods for discretization of the surface Stokes equation. Both methods use the same penalty approach for treating the tangential flow constraint and the same Taylor-Hood \mathbf{P}_k-P_{k-1} spaces. For a higher order geometry approximation the parametric trace finite

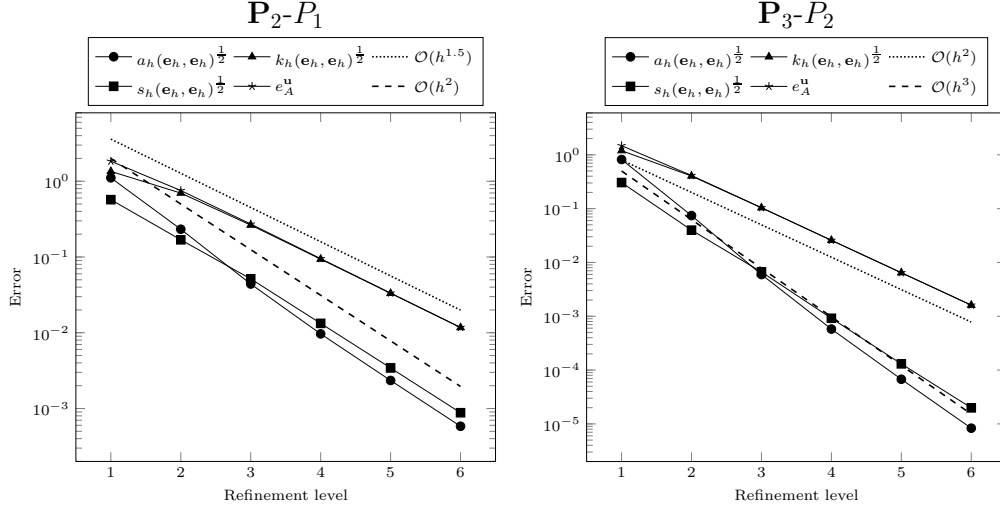


Fig. 7.6: Components of the energy norm error for (P2h)

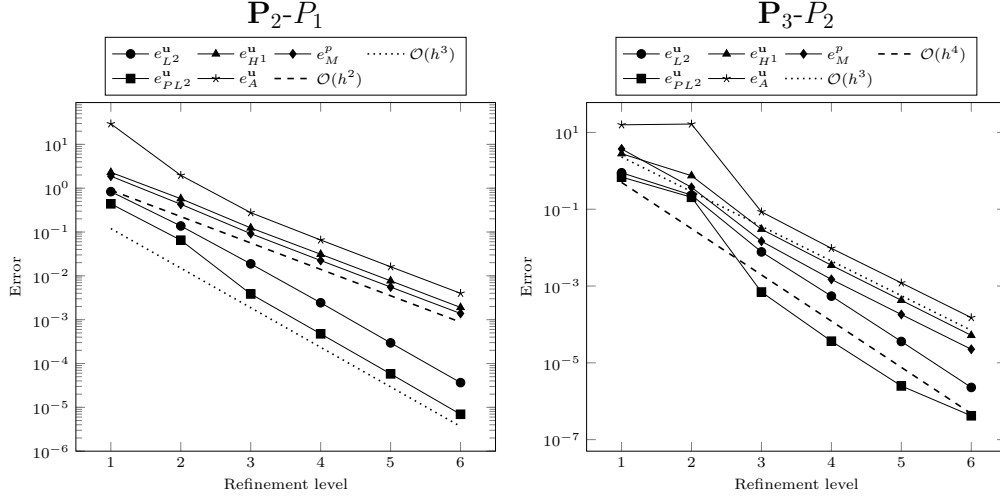


Fig. 7.7: Consistent formulation (P1h) on the torus

element technique is used. For the parameters in these methods specific choices are proposed. The numerical experiments show that for $k = 2$ and $k = 3$ the resulting methods have optimal convergence orders in the $H^1(\Gamma_h)$ - and $L^2(\Gamma_h)$ -norm. For the consistent method (P1h) an approximation of the Weingarten map has to be determined, which is not needed in the inconsistent method (P2h). For the consistent method and $k = 2$ an optimal order discretization error bound for the case $\Gamma_h = \Gamma$ (i.e., no geometry errors) is derived in [27]. For the inconsistent method a rigorous

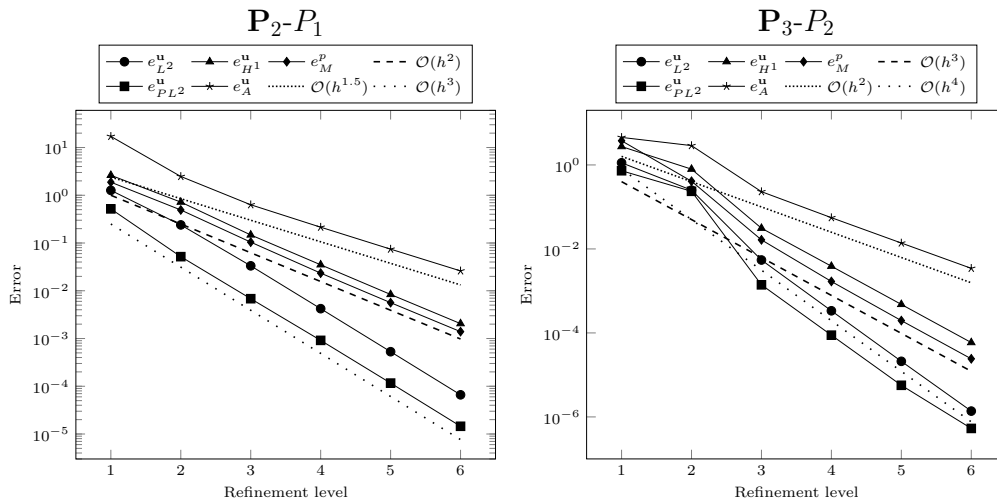


Fig. 7.8: Inconsistent formulation (P2h) on the torus

optimal error bound is not available, yet.

In future work these methods will be applied to other related problem classes, e.g., time dependent surface Navier-Stokes equations, and compared to other methods. Furthermore, the analysis can be extended in several directions, for example, by including geometry errors and deriving (optimal) error bounds also for the inconsistent method.

REFERENCES

- [1] *Netgen/NGSolve*. <https://ngsolve.org/>.
- [2] M. ARROYO AND A. DESIMONE, *Relaxation dynamics of fluid membranes*, Phys. Rev. E, 79 (2009), p. 031915.
- [3] A. BONITO, A. DEMLOW, AND M. LICHT, *A divergence-conforming finite element method for the surface Stokes equation*, arXiv:1908.11460, (2019).
- [4] A. BONITO, A. DEMLOW, AND R. H. NOCHETTO, *Finite element methods for the Laplace-Beltrami operator*, arXiv:1906.02786, (2019).
- [5] E. BURMAN, S. CLAUS, P. HANSBO, M. G. LARSON, AND A. MASSING, *Cutfem: Discretizing geometry and partial differential equations*, International Journal for Numerical Methods in Engineering, 104 (2015), pp. 472–501.
- [6] E. BURMAN, P. HANSBO, M. G. LARSON, AND A. MASSING, *Cut finite element methods for partial differential equations on embedded manifolds of arbitrary codimensions*, ESAIM: Mathematical Modelling and Numerical Analysis, 52 (2018), pp. 2247–2282.
- [7] A. DEMLOW, *Higher-order finite element methods and pointwise error estimates for elliptic problems on surfaces*, SIAM J. Numer. Anal., 47 (2009), pp. 805–827.
- [8] G. DZIUK AND C. M. ELLIOTT, *Finite element methods for surface PDEs*, Acta Numerica, 22 (2013), pp. 289–396.
- [9] D. G. EBIN AND J. MARSDEN, *Groups of diffeomorphisms and the motion of an incompressible fluid*, Annals of Mathematics, 92 (1970), pp. 102–163.
- [10] T.-P. FRIES, *Higher-order surface FEM for incompressible Navier-Stokes flows on manifolds*, International Journal for Numerical Methods in Fluids, 88 (2018), pp. 55–78.
- [11] J. GRANDE, C. LEHRENFELD, AND A. REUSKEN, *Analysis of a high-order trace finite element*

- method for PDEs on level set surfaces*, SIAM Journal on Numerical Analysis, 56 (2018), pp. 228–255.
- [12] M. E. GURTIN AND A. I. MURDOCH, *A continuum theory of elastic material surfaces*, Archive for Rational Mechanics and Analysis, 57 (1975), pp. 291–323.
- [13] P. HANSBO, M. G. LARSON, AND K. LARSSON, *Analysis of finite element methods for vector Laplacians on surfaces*, IMA Journal of Numerical Analysis, (2019).
- [14] T. JANKUHN, M. A. OLSHANSKII, AND A. REUSKEN, *Incompressible fluid problems on embedded surfaces: Modeling and variational formulations*, Interfaces and Free Boundaries, 20 (2018), pp. 353–377.
- [15] T. JANKUHN AND A. REUSKEN, *Trace finite element methods for surface vector-Laplace equations*, arXiv:1904.12494, (2019).
- [16] H. KOKA, C. LIU, AND Y. GIGA, *Energetic variational approaches for incompressible fluid systems on an evolving surface*, Quart. Appl. Math., 75 (2017), pp. 359–389.
- [17] P. L. LEDERER, C. LEHRENFELD, AND J. SCHÖBERL, *Divergence-free tangential finite element methods for incompressible flows on surfaces*, arXiv:1909.06229, (2019).
- [18] C. LEHRENFELD, *ngsxfem*. <https://github.com/ngsxfem>.
- [19] C. LEHRENFELD, *High order unfitted finite element methods on level set domains using isoparametric mappings*, Computer Methods in Applied Mechanics and Engineering, 300 (2016), pp. 716–733.
- [20] C. LEHRENFELD AND A. REUSKEN, *Analysis of a high-order unfitted finite element method for elliptic interface problems*, IMA Journal of Numerical Analysis, 38 (2017), pp. 1351–1387.
- [21] M. MITREA AND M. TAYLOR, *Navier-Stokes equations on Lipschitz domains in Riemannian manifolds*, Mathematische Annalen, 321 (2001), pp. 955–987.
- [22] T.-H. MIURA, *On singular limit equations for incompressible fluids in moving thin domains*, Quart. Appl. Math., 76 (2018), pp. 215–251.
- [23] I. NITSCHKE, S. REUTHER, AND A. VOIGT, *Hydrodynamic interactions in polar liquid crystals on evolving surfaces*, Phys. Rev. Fluids, 4 (2019), p. 044002.
- [24] I. NITSCHKE, A. VOIGT, AND J. WENSCH, *A finite element approach to incompressible two-phase flow on manifolds*, Journal of Fluid Mechanics, 708 (2012), pp. 418–438.
- [25] M. A. OLSHANSKII, A. QUAINI, A. REUSKEN, AND V. YUSHUTIN, *A finite element method for the surface Stokes problem*, SIAM Journal on Scientific Computing, 40 (2018), pp. A2492–A2518.
- [26] M. A. OLSHANSKII AND A. REUSKEN, *Trace finite element methods for PDEs on surfaces*, in Geometrically Unfitted Finite Element Methods and Applications, S. P. A. Bordas, E. Burman, M. G. Larson, and M. A. Olshanskii, eds., Cham, 2017, Springer International Publishing, pp. 211–258.
- [27] M. A. OLSHANSKII, A. REUSKEN, AND A. ZHILIAKOV, *Inf-sup stability of the trace P_2 - P_1 Taylor-Hood elements for surface PDEs*, Preprint arXiv:1909.02990, (2019).
- [28] M. A. OLSHANSKII AND V. YUSHUTIN, *A penalty finite element method for a fluid system posed on embedded surface*, Journal of Mathematical Fluid Mechanics, 21 (2019), p. 14.
- [29] A. REUSKEN, *Analysis of trace finite element methods for surface partial differential equations*, IMA Journal of Numerical Analysis, 35 (2015), pp. 1568–1590.
- [30] ———, *Stream function formulation of surface Stokes equations*, IMA Journal of Numerical Analysis, (2018).
- [31] S. REUTHER AND A. VOIGT, *The interplay of curvature and vortices in flow on curved surfaces*, Multiscale Modeling & Simulation, 13 (2015), pp. 632–643.
- [32] ———, *Solving the incompressible surface Navier-Stokes equation by surface finite elements*, Physics of Fluids, 30 (2018), p. 012107.
- [33] J. SCHÖBERL, *Netgen an advancing front 2d/3d-mesh generator based on abstract rules*, Computing and Visualization in Science, 1 (1997), pp. 41–52.
- [34] M. E. TAYLOR, *Analysis on Morrey spaces and applications to Navier-Stokes and other evolution equations*, Communications in Partial Differential Equations, 17 (1992), pp. 1407–1456.
- [35] R. TEMAM, *Infinite-dimensional dynamical systems in mechanics and physics*, Springer, New York, 1988.